Optical Properties of Cadmium Sulfide Clusters

Jan-Ole Joswig,*,† Gotthard Seifert,‡ Thomas A. Niehaus,§ and Michael Springborg†

Physikalische Chemie, Universität des Saarlandes, D-66123 Saarbrücken, Germany, Institut für Physikalische Chemie und Elektrochemie, Technische Universität Dresden, D-01062 Dresden, Germany, and Fachbereich 6−Physik, Universität-GH Paderborn, D-33098 Paderborn, Germany

Received: August 13, 2002; In Final Form: November 19, 2002

Using a time-dependent extension of a density-functional tight-binding method, we have calculated the excitation spectra of stoichiometric cadmium sulfide clusters up to 144 atoms. The spectra show a strong dependency of the lowest unoccupied molecular orbitals on the structural properties of the clusters, especially on the number of single-bonded surface atoms. Furthermore, we calculated the single-particle energy eigenvalues for a number of clusters up to 440 atoms without structural relaxation. Here, with increasing cluster size the gap between highest occupied and lowest unoccupied molecular orbitals (HOMO/LUMO gap) is decreasing asymptotically toward the bulk band gap of cadmium sulfide for clusters with no single-bonded surface atoms and tending to a zero gap for clusters with a large number of single-bonded surface cadmium atoms. The latter is caused by low-lying cadmium 5s states.

1. Introduction

Semiconductor clusters and nanoparticles have become intensively investigated fields by both experimentalists and theoreticians in the past two decades. One reason for the increasing interest in semiconductor nanoparticles is their electronic and optical properties that can be tuned by varying the size of the particles. This feature is referred to as a quantum confinement effect or a quantum size effect (QSE)[1−5] and can be considered to be an experimental realization of the particle in a box. This theoretical problem occurs if a particle, for example, an electron, is trapped in confined dimensions. The confinement may appear in one, two, or all three dimensions. Experimentally, these possible confinements are observed as quantum wells, quantum wires, or quantum dots, respectively. In a confined system, for example, a cluster or nanoparticle, the gaps between single energy levels (e.g., the HOMO/LUMO gap) increase with decreasing system size (i.e., increasing confinement). However, with increasing system size, the spacings between energy levels are reduced; moreover, the number of levels rises as the number of particles also increases. More and more the system takes over bulk properties (e.g., the development of bands instead of discrete energy levels). Experimentally, nanoparticles therefore have a HOMO/LUMO gap that is higher than the bulk band gap. With increasing particle size, the value of the gap approaches the bulk band gap from above.

II-VI semiconductors such as cadmium sulfide, selenide, and telluride are especially interesting because they have different possible crystal structures such as zinc blende and wurtzite. For some compounds, there even exists the high-pressure rock salt crystal structure.[6,7] For cadmium sulfide, the first two crystal structures, zinc blende and wurtzite, are energetically almost degenerate in the bulk, with the wurtzite structure being slightly more stable.[8,9] This raises the question of whether clusters of zinc blende- or wurtzite-derived structures will be more stable or if the crystal structure does not play any role at all in the stability of these clusters. We investigated this question elsewhere.[10]

In some of the studies of cadmium sulfide, selenide, or telluride clusters, the effective-mass method has been applied to calculate the energetically lowest optical transitions.[11−15] Thereby, the underlying structure of the cluster becomes of only secondary importance. Alternatively, tight-binding methods have also been applied to these systems,[16−29] and it has almost exclusively been assumed that the structure of the cluster is that of a finite part of the infinite crystal structure. The structural relaxation has not been taken into account in most of these studies except one by Whaley and co-workers,[28] who used an sp^3s^* tight-binding model, and the density-functional work by Ahlrichs et al.[30,31] Chelikowsky et al.[32] performed TDLDA calculations of small Cd_nSe_n clusters ($n \leq 8$) whose structures have been obtained using a simulated annealing strategy.[33] The clusters of that study are, however, small, whereas we examine in this work—to our knowledge for the first time—the optical properties of larger clusters systematically.

In the present work, we shall explicitly study how the electronic and optical properties of stoichiometric Cd_nS_n clusters depend on n. We therefore calculated excitation spectra for clusters with n up to approximately 70 and single-particle energies for clusters with n up to approximately 220. For all of the clusters, we considered spherical parts of both zinc blende and wurtzite crystals. The structures for calculating the spectra have been relaxed to the closest local-energy minimum as a first step. Thereby, all atoms have been allowed to move. The center of the initial spherical structures was chosen to be the midpoint of a Cd−S nearest-neighbor bond. This guarantees the stoichiometry of all of the clusters.

The article is organized as follows: in section 2, the computational methods are described; the results are presented in section 3; and a brief summary of our conclusions is given in section 4.

* Corresponding author. E-mail: j.joswig@mx.uni-saarland.de.
† Universität des Saarlandes.
‡ Technische Universität Dresden.
§ Universität-GH Paderborn.

10.1021/jp026752s CCC: $25.00 © 2003 American Chemical Society
Published on Web 03/08/2003

2. Computational Methods

The calculational electronic-structure method has been described in detail elsewhere.[34] The density-functional tight-binding method (DFTB) has also been used for the structural optimization of the clusters. Furthermore, we used an extension[35] performing within time-dependent density-functional response theory (TD-DFRT) for the calculations of the excitation spectra. The calculations performed by this program package will be referred to as TD-DFRT-TB.[36] Here, we give a brief overview of the methods and refer the reader who is interested in more details to those references.

The DFTB method is based on the density functional theory of Hohenberg and Kohn[37] in the formulation of Kohn and Sham.[38] The single-particle Kohn−Sham eigenfunctions $\psi_i(\mathbf{r})$ are expanded in a suitable set of localized atomiclike basis functions $\varphi_m(\mathbf{r})$. These functions are determined by self-consistent density-functional calculations on the isolated atoms employing a large set of Slater-type basis functions.

Furthermore, we make use of a tight-binding approximation, so that

$$h_{mn} = \langle\varphi_m|\hat{t} + \sum_j V_j^0|\varphi_n\rangle = \langle\varphi_m|\,\hat{t} + V_{j_m}^0 + (1-\delta_{j_n,j_m})V_{j_n}^0|\,\varphi_n\rangle \quad (1)$$

where the mth and nth basis functions φ_m and φ_n are centered on the atoms at $\mathbf{R}_{j_m}$ and $\mathbf{R}_{j_n}$, respectively, $\hat{t}$ is the kinetic-energy operator, and V_j^0 are the potentials of the neutral atoms superposed to approximate the effective Kohn−Sham potential. Through the approximation of eq 1, only two-center terms in the Hamiltonian matrix are considered, but all two-center terms (i.e., $h_{mn} = \langle\varphi_m|\hat{h}|\varphi_n\rangle$, $S_{mn} = \langle\varphi_m|\varphi_n\rangle$) are calculated exactly.

The approximations lead to the same structure of the secular equations

$$\sum_m c_{im}(h_{mn} - \epsilon_i S_{mn}) = 0 \quad (2)$$

as in other (nonorthogonal) tight-binding schemes, but it is important to stress that all matrix elements are calculated and none is determined through fitting to experimental results.

Since the difference between superposed atomic electron densities and the true electron density of the system of interest is small and since by far the largest parts of the interatomic interactions are of fairly short range, the major part of the binding energy is contained in the difference of the single-particle energies of the system of interest, $\{\epsilon_i\}$, and of the isolated atoms, $\{\epsilon_{jm_j}\}$ (j being an atom index, and m_j an orbital index):

$$\epsilon_B \equiv \sum_i^{occ}\epsilon_i - \sum_j\sum_{m_j}\epsilon_{jm_j} \quad (3)$$

The short-ranged interactions can be approximated by simple pair potentials so that we end up with the following expression for the binding energy:

$$E_B \approx \epsilon_B + \frac{1}{2}\sum_{j\neq j'} U_{jj'}(|\mathbf{R}_j - \mathbf{R}_{j'}|) \quad (4)$$

$U_{jj'}(|\mathbf{R}_j - \mathbf{R}_{j'}|)$ is determined as the difference of ϵ_B and E_B^{SCF} for diatomic molecules with E_B^{SCF} being the total energy from parameter-free density-functional calculations (i.e., in our study of CdS, Cd_2, and S_2).

Finally, all electrons except for the 5s and 4d electrons of cadmium and the 3s and 3p electrons of sulfur were treated within a frozen-core approximation.

As mentioned above, the time-dependent extension of the DFTB scheme will be referred to as TD-DFRT-TB. To obtain the excitation energies, the coupling matrix, which gives the response of the potential with respect to a change in the electron density, has to be built. It has the following form:[39,40]

$$K_{ij\sigma,kl\tau} = \int\int \psi_i(\mathbf{r})\,\psi_j(\mathbf{r})\left(\frac{1}{|\mathbf{r}-\mathbf{r}'|} + \frac{\delta^2 E_{xc}}{\delta\rho_\sigma(\mathbf{r})\,\delta\rho_\tau(\mathbf{r}')}\right)\psi_k(\mathbf{r}')\,\psi_l(\mathbf{r}')\,d\mathbf{r}\,d\mathbf{r}' \quad (5)$$

σ and τ are spin indices, E_{xc} is the exchange-correlation energy, and ρ is the electron density. By solving the eigenvalue problem

$$\sum_{ij\sigma}\left[\omega_{ij}^2\delta_{ik}\delta_{jl}\delta_{\sigma\tau} + 2\sqrt{\omega_{ij}}K_{ij\sigma,kl\tau}\sqrt{\omega_{kl}}\right]F_{ij\sigma}^I = \omega_I^2\,F_{kl\tau}^I \quad (6)$$

the true excitation energies ω_I are obtained ($\omega_{ij} = \epsilon_j - \epsilon_i$, where i, k are occupied Kohn−Sham orbitals, whereas j, l are unoccupied ones).

The coupling matrix of eq 5 is now approximated (γ approximation) to

$$K_{ij\sigma,kl\tau} = \sum_{\alpha\beta} q_{ij\alpha}q_{kl\beta}[\tilde{\gamma}_{\alpha\beta} + (2\delta_{\sigma\tau} - 1)m_{\alpha\beta}] \quad (7)$$

where

$$\tilde{\gamma}_{\alpha\beta} = \int\int f_{uxc}[\mathbf{r},\mathbf{r}',\rho]F_\alpha(\mathbf{r})F_\beta(\mathbf{r}')\,d\mathbf{r}\,d\mathbf{r}' \quad (8)$$

$$m_{\alpha\beta} = \int\int \left.\frac{\delta^2 E_{xc}}{\delta m(\mathbf{r})\,\delta m(\mathbf{r}')}\right|_\rho F_\alpha(\mathbf{r})F_\beta(\mathbf{r}')\,d\mathbf{r}\,d\mathbf{r}' \quad (9)$$

with $q_{ij\alpha}$ being the Mulliken atomic transition charge

$$q_{ij\alpha} = \frac{1}{2}\sum_{\mu\in\alpha}\sum_\nu [c_{i\mu}c_{j\nu}S_{\mu\nu} + c_{i\nu}c_{j\mu}S_{\nu\mu}] \quad (10)$$

and $F_\alpha(\mathbf{r})$ being a normalized spherical density distribution on atom α. f_{uxc} is shorthand for the integral kernel in eq 5 in the spin-independent part, whereas $m_{\alpha\beta}$ considers the spin-dependent part with the magnetization densities $m(\mathbf{r})$. The on-site term $\tilde{\gamma}_{\alpha\alpha}$ can be approximated by a Hubbard-like term $\tilde{U}_\alpha$, which can be calculated from the second derivative of the total energy with respect to the occupation number of the highest occupied atomic orbital. Because the term in eq 9 is of very short-ranged nature, we take it as strictly on-site ($m_{\alpha\beta} = 0$ for $\alpha \neq \beta$, $m_{\alpha\alpha} \equiv M_\alpha$). With this approximation and by neglecting charge-transfer effects, M_α is obtained from atomic DFT calculations:

$$M_\alpha = \frac{1}{2}\left(\frac{\partial\epsilon_\uparrow^{HOMO}}{\partial\rho_\uparrow} - \frac{\partial\epsilon_\uparrow^{HOMO}}{\partial\rho_\downarrow}\right) \quad (11)$$

$\rho_\uparrow$ and $\rho_\downarrow$ are the spin-up and spin-down densities, respectively. These approximations allow an efficient calculation of the coupling matrix of eq 7. The excitation energies determined by eq 6 and the required singlet oscillator strength can be calculated using

$$f^I = \frac{2}{3}\omega_I \sum_{k=x,y,z} \left| \sum_{ij} \langle \psi_i | r_k | \psi_j \rangle \sqrt{\frac{\omega_{ij}}{\omega_I}} (F^I_{ij\uparrow} + F^I_{ij\downarrow}) \right|^2 \quad (12)$$

with the transition-dipole matrix elements

$$\langle \psi_i | \mathbf{r} | \psi_j \rangle = \sum_\alpha \mathbf{R}_\alpha q_{ij\alpha} \quad (13)$$

3. Results

Figure 1 shows the calculated spectra of 10 cadmium sulfide clusters. More spectra of up to 72 CdS pairs (144 atoms) have been calculated but are not shown here because the trends may be seen from the displayed spectra as well. One of the eye-catching features of the Figure is the variation of the lowest-energy transition. Six out of 10 clusters show a smallest excitation energy of about 1.6−1.8 eV. The other four have a much higher excitation energy of more than 3 eV. The variation is observed in both zinc blende- and wurtzite-derived structures. The spectra even show similarities for clusters of different structure types (zinc blende, wurtzite) but the same number of atoms (e.g., the two intense low-lying onset peaks in the spectra of $Cd_{16}S_{16}$). Therefore, the main crystal structure has only a marginal influence on the absorption spectrum of a cluster, especially on the size of the HOMO/LUMO gap.

Nevertheless, the spectra show a strong dependency on the number of atoms that the clusters contain. This is, of course, also a structural feature. The influence of the cluster size can be seen very clearly in the spectra of the two wurtzite-derived clusters $Cd_{16}S_{16}$ and $Cd_{17}S_{17}$. By adding just one extra pair of atoms, the HOMO/LUMO gap is doubled. In respect thereof, the size dependency of the calculated spectra is enormous and shall be investigated below.

Figure 2 displays the two structures of $Cd_{16}S_{16}$ and $Cd_{17}S_{17}$ derived from the wurtzite crystal structure. Each of the two atoms of the additional pair in $Cd_{17}S_{17}$ is capping one group of three atoms that have just a single bond in $Cd_{16}S_{16}$. Therefore, the main structural difference of the two clusters is the number of single-bonded atoms—six in $Cd_{16}S_{16}$ and none in $Cd_{17}S_{17}$. Table 1 compares the calculated lowest excitation energies (TD-DFRT-TB) with the number of single-bonded atoms per cluster. The correlation of the HOMO/LUMO gap and the existence of single-bonded atoms is obvious. Clusters without any single-bonded surface atoms have gaps of more than 3 eV, whereas all other clusters have much lower HOMO/LUMO gaps. This feature is independent of the crystal structure that the clusters are derived from (i.e., zinc blende or wurtzite). As we have already shown in a previous work,[10] the HOMO in the clusters is rather delocalized over the whole cluster, whereas the LUMO is localized at surface atoms. This is nicely illustrated for the $Cd_{68}S_{68}$ cluster (displayed in Figure 3). This cluster has a particularly large number of single-bonded surface atoms—10 sulfur atoms plus 10 cadmium atoms. The calculated density of states is shown in Figure 4. After subtracting the contributions of all single-bonded surface atoms, we find that the peak in the density of states above the Fermi energy at about 1.5 eV does nearly vanish. The remaining spectrum now has a lowest-energy transition at about 3 eV, which is higher than the experimental CdS bulk absorption at 2.58 eV[41] and, therefore, in good agreement with the theory of the particle in a box. A detailed analysis of the contributions of the surface atoms to the density of states around the Fermi energy is given in Figure 5. This Figure shows the total density of states as well as the projected local densities of states for a bulk and a single-bonded surface

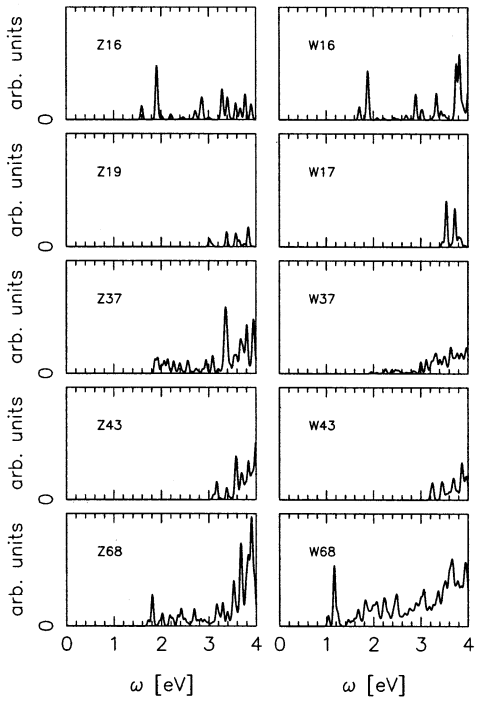

Figure 1. TD-DFRT-TB spectra of zinc blende- (left column) and wurtzite- (right column) derived CdS clusters. The caption of each diagram states the original crystal structure that the cluster is derived from (Z: zinc blende; W: wurtzite) and the number CdS pairs. All *y* axes have the same scale, and all curves are broadened with Gaussians (0.27 eV).

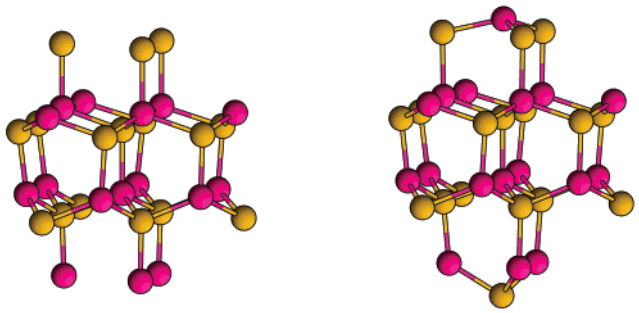

Figure 2. Wurtzite-derived CdS clusters with 16 (left) and 17 (right) CdS pairs. Cadmium atoms are shown as pink spheres, and sulfur atoms as gold spheres.

cadmium atom. It can be seen clearly that the surface cadmium atom contributes very much to the first unoccupied states between 0 and 4 eV. In particular, the contribution of s and p states is high. The sulfur atoms do not contribute. The local density of states of the bulk cadmium atom does not show any contribution below 6 eV. The consequence of the different local densities of states of structurally different cadmium atoms is that the HOMO/LUMO gap of clusters with one or more single-bonded atoms is reduced by the surface states of these atoms. These results are in agreement with a theoretical investigation of InP quantum dots by Zunger et al.[42] in which the authors observed the same low-lying surface state for nonpassivated nanoparticles and their absence for the passivated ones.

A collective feature of all of the calculated spectra with small HOMO/LUMO gaps (i.e., those with a large number of unsaturated (cadmium) atoms) is the high intensity of the first peak—see Figure 1. This intense excitation cannot be found in the corresponding joint density of states (Figure 6). It is evidence that these intense low-lying excitations are obviously due to an

TABLE 1: Excitation Energies and Number of Single-Bonded Atoms[a]

no. of CdS pairs	gap [eV]	no. of single atoms
W04	3.58	0
W10	3.15	0
W16	1.70	6
W17	3.46	0
W26	1.95	6
W37	1.95	1
W43	3.21	0
W51	1.91	2
W57	1.92	2
W68	1.03	20
W72	1.80	6
Z04	2.16	6
Z10	3.82	0
Z16	1.60	6
Z19	3.02	0
Z28	1.79	12
Z37	1.87	6
Z43	3.10	0
Z57	1.36	8
Z65	3.11	0
Z68	1.72	6

[a] The first column displays the structure (Z: zinc blende, W: wurtzite) and the number of CdS pairs per cluster, the second column contains the calculated lowest-energy excitation (by TD-DFRT-TB), and the last column displays the number of single-bonded surface atoms.

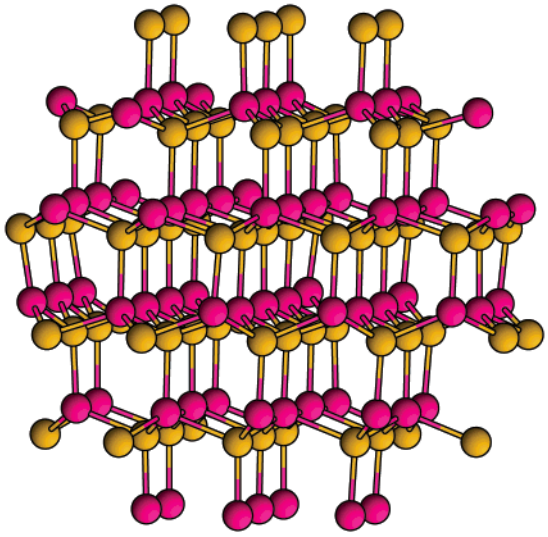

Figure 3. $Cd_{68}S_{68}$ cluster of wurtzite-derived structure. Cadmium atoms are shown as pink spheres, and sulfur atoms as gold spheres.

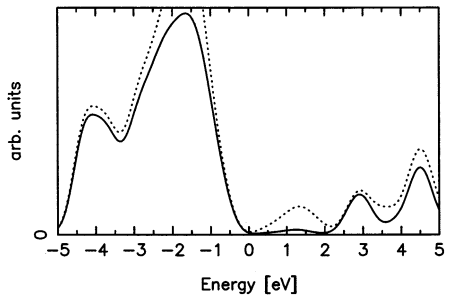

Figure 4. Total density of states of $Cd_{68}S_{68}$ (···) and total density of states (—) after subtracting the contributions of 20 single-bonded surface atoms (10 cadmium and 10 sulfur atoms). The curves are broadened with Gaussians (0.27 eV). The Fermi level is at 0 eV.

excitation of a collective mode that resembles the well-known surface plasmon excitations observed, for example, in metal clusters.[43]

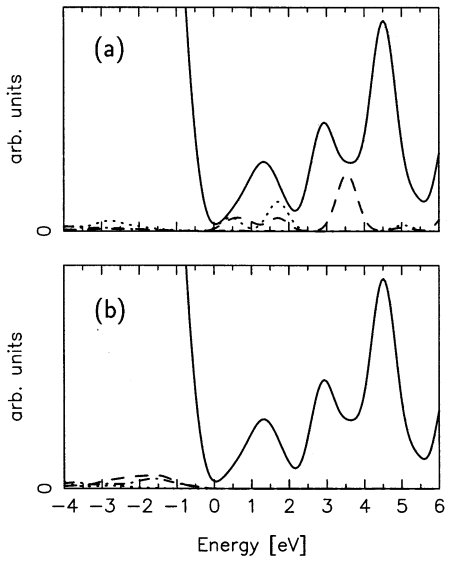

Figure 5. Total density of states (—) and s (···), p (— —), and d contributions (— · —) of the atom to the total density of states (scaled by a factor of 7.2) for (a) a surface single-bonded atom and (b) a bulk cadmium atom. All curves are broadened with Gaussians (0.27 eV). The Fermi level is at 0 eV.

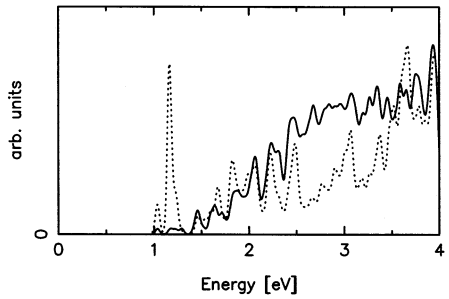

Figure 6. TD-DFRT-TB spectrum (···) and joint density of states (—) of the wurtzite-derived $Cd_{68}S_{68}$ cluster. Both curves are broadened with Gaussians (0.27 eV) and scaled to be visualized in one diagram.

We shall now take a closer look at the calculated TD-DFRT-TB spectra of Figure 1 compared to the single-particle excitation energies. To compare these two, we display in Figure 6 the TD-DFRT-TB spectrum of $Cd_{68}S_{68}$ together with the joint density of states of the same cluster obtained from the single-particle energy eigenvalues. Both curves have similar features (e.g., the lowest-energy peaks) but differ, of course, in the intensities because the joint density of states does not take into account any selection rules or collective effects.

An additional similarity of both curves is their onset peak. The TD-DFRT-TB spectrum does not show any shift of the lowest-energy transition compared to the joint density of states. On first view, this seems to be unusual and may point to an error within the calculational scheme. But if we have a look at other calculations of this type,[31,44] we see similar results. Ahlrichs et al.[31] performed calculations of cadmium selenide clusters, which are strongly related not only structurally but also electronically to the cadmium sulfide clusters investigated in this work. Their calculated TDLDA spectra also feature the same lowest-energy transition as observed in the density of states. Moreover, these transitions tend to be too small for larger clusters. In our opinion, the HOMO/LUMO gaps that are too small arise mainly from low-lying unoccupied cadmium 5s states rather than from computational artifacts. Also, experimental data gives evidence for these low-lying surface states.[45] Unfortunately, a quantitative comparison of our results to the afore-

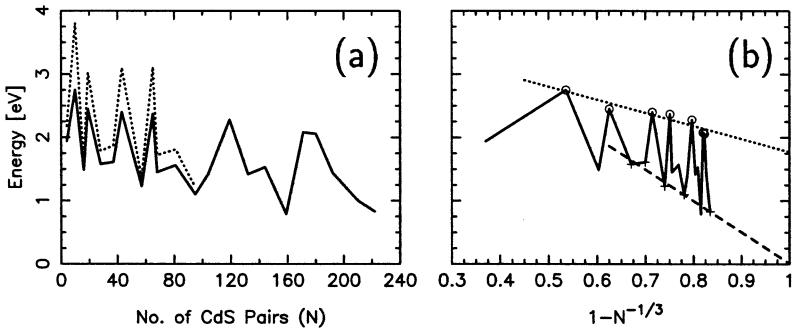

Figure 7. (a) HOMO/LUMO gap as a function of cluster size for zinc blende-derived clusters. The gap is taken from spherical cutouts of the zinc blende crystal structures (—) and for optimized structures of these clusters (···). (b) HOMO/LUMO gap as function of $1 - N^{-1/3}$ (with N being the number of CdS pairs). The gap corresponds to the unrelaxed structures in the left panel (—). Trend lines are drawn through the gap maxima (dotted, open circles) and minima (dashed, plus signs, excluding the two smallest clusters) to accentuate the size dependence of the HOMO/LUMO gap.

mentioned theoretical work is not possible because the exact cluster sizes are not indicated. Chelikowsky et al.[32,33] give the precise sizes, but their clusters are much smaller than those studied in this work and, therefore, are also not comparable.

After analyzing the optical and electronic properties of some single cadmium sulfide clusters, the size dependence of these properties will now be discussed in more detail. In Figure 7, the HOMO/LUMO gaps of zinc blende-derived clusters are displayed as a function of size. Clusters up to 222 CdS pairs (444 atoms) have been calculated. The calculations of the single-particle energy eigenvalues have been made for the nonrelaxed spherical cutouts of the crystal structure. For comparison, the gaps calculated for the optimized smaller clusters (up to 95 CdS pairs) are also shown. As can be seen, the relaxation does not have a great influence on the trend in the size of the HOMO/LUMO gap, but for clusters with relatively large gaps on average, the gap size is increased by about 0.8 eV on average after optimizing the structures. The oscillations in the size dependence of the HOMO/LUMO gap are mainly due to the varying structure and number of single-bonded surface atoms. But overall, the curve is decreasing. This was found by other groups also.[16,20,25,46,47] In the right panel of Figure 7, we have drawn the calculated gap-size dependence on $1 - N^{-1/3}$, with N being the number of CdS pairs in the cluster. This plot accentuates the size dependence of the gap size. A trend line along the points for clusters with relatively large gaps roughly confirms the size dependence as it is expected for a particle in a box and also observed, for example, in CdSe nanoparticles.[48] The extrapolation leads to a bulk limit ($1 - N^{-1/3} \rightarrow 1$) of 1.75 eV; considering the upward shift of 0.8 eV due to structure relaxation, as mentioned above, this extrapolated gap size matches the experimental value of the bulk band gap (2.58 eV[41]). In contrast to this result, a corresponding trend line along the gap minima, excluding the two smallest clusters, asymptotically goes to a zero gap (i.e., metallic behavior). This result supports the abovementioned character of the surface states in clusters with unsaturated cadmium surface atoms. In the case of very large particles, this would lead to a metalliclike surface shell if the metal atoms would not be "passivated" with organic ligands.

After all, the surface atoms have a very strong influence on the optical and electronic properties of the investigated cadmium sulfide clusters. Clusters of the investigated sizes (i.e., those with diameters of up to a few nanometers) have a surface-to-bulk ratio that is much too high to show arising bulk properties. These may appear in nanoparticles with diameters of some tens to hundreds of nanometers, but in the cluster range, the dependency on surface effects is still high.

4. Conclusions

In the present work, we have applied a simplified LCAO-DFT-LDA scheme and its time-dependent extension (TD-DFRT-TB) to study the optical and electronic properties of stoichiometric cadmium sulfide clusters up to 144 atoms. To our knowledge, this work represents the first systematic study of the optical properties including the TD-DFRT-TB spectra of semiconductor clusters.

By comparing the calculated TD-DFRT-TB spectra to the joint densities of states, we did not observe any shift of the lowest-energy transitions. This is in agreement with the work of Ahlrichs et al.,[31] but the spectra show strong fluctuations in the onset energies depending on the structural properties of the clusters, in particular, on the number of single-bonded atoms at the surface. By subtracting the local density of states of the single-bonded atoms, we obtain a different spectrum with a gap of about 3 eV. The additional states below this value arise from the cadmium 5s levels of the single-bonded surface atoms. Other surface atoms also contribute but by a much smaller amount. There is also experimental evidence for the surface localization of the LUMO. Bawendi et al.[45] observed that one or both charge carriers of the exciton are trapped and localized on the surface. The presence and importance of these surface states in nanoparticles reveal a fundamental difference between dispersed spherical semiconductor clusters and films that have epitaxial surfaces.

The intense low-lying excitations of spectra of clusters with a large number of unsaturated cadmium atoms indicate that these excitations may be of a collective mode. These are observed experimentally in metal clusters as surface plasmon excitations.[43]

The HOMO/LUMO gap as a function of size shows strong oscillations according to the discussed surface dependency of the LUMO. Moreover, it decreases with increasing cluster size. The gap values lie below the experimental bulk band gap for unrelaxed structures. Low-lying cadmium 5s levels close the gap of clusters with a large number of single-bonded surface atoms.

The influence of the surface is very important for cadmium sulfide and other semiconductor clusters with diameters of just a few nanometers. The comparison to experimental data is difficult because there are only a few results for such small clusters. Another difficulty arises from the way spectra are recorded. In solutions, the surface states obtained in theoretical calculations of naked clusters do not occur because the clusters are mostly dispersed in Lewis-base organic solvents (e.g., tributyl phosphane[45]). This type of solvent complexes and most likely passivates the surface metal (i.e., cadmium) atoms.

Calculations of clusters covered by such organic molecules

may be a pathway of further theoretical investigations of the optical properties. Although this will be much more time-consuming, the results would be much easier to compare to experimental obtained spectra.

Acknowledgment. M.S. is grateful to Fonds der Chemischen Industrie for very generous support. Furthermore, this work was supported by SPP 1072 of the Deutsche Forschungsgemeinschaft.

References and Notes

(1) Henglein, A. In *Topics in Current Chemistry*; Steckhan, E., Ed.; Springer-Verlag: Berlin, 1988; Vol. 143, p 113.
(2) Yoffe, A. D. *Adv. Phys.* **1993**, *42*, 173.
(3) Nirmal, M.; Norris, D. J.; Kuno, M.; Bawendi, M. G.; Efros, A. L.; Rosen, M. *Phys. Rev. Lett.* **1995**, *75*, 3728.
(4) Alivisatos, A. P. *J. Phys. Chem.* **1996**, *100*, 13226.
(5) Gorer, S.; Hodes, G. In *Semiconductor Nanoclusters*; Kamat, P. V., Meisel, D., Eds.; Elsevier Science B. V.: Amsterdam, 1996.
(6) Desgreniers, S. *Phys. Rev. B* **1998**, *58*, 14102.
(7) Recio, J. M.; Blanco, M. A.; Luaña, V.; Pandey, R.; Gerward, L.; Staun Olsen, J. *Phys. Rev. B* **1998**, *58*, 8949.
(8) Yeh, C. Y.; Lu, Z. W.; Froyen, S.; Zunger, A. *Phys Rev. B* **1992**, *45*, 12130.
(9) Federov, V. A.; Ganshin, V. A.; Korkishko, Y. N. *Mater. Res. Bull.* **1993**, *28*, 59.
(10) Joswig, J.-O.; Springborg, M.; Seifert, G. *J. Phys. Chem. B* **2000**, *104*, 2617.
(11) Brus, L. E. *J. Chem. Phys.* **1983**, *79*, 5566.
(12) Brus, L. E. *J. Chem. Phys.* **1984**, *80*, 4403.
(13) Schmidt, H. M.; Weller, H. *Chem. Phys. Lett.* **1986**, *129*, 615.
(14) Ekimov, A. I.; Efros, A. L.; Ivanov, M. G.; Onushchenko, A. A.; Shumilov, S. K. *Solid State Commun.* **1989**, *69*, 565.
(15) Einevoll, G. T. *Phys. Rev. B* **1992**, *45*, 3410.
(16) Lippens, P. E.; Lannoo, M. *Phys. Rev. B* **1989**, *39*, 10935.
(17) Rama Krishna, M. V.; Friesner, R. A. *J. Chem. Phys.* **1991**, *95*, 8309.
(18) Hill, N. A.; Whaley, K. B. *J. Chem. Phys.* **1994**, *100*, 2831.
(19) Tomasulo, A.; Ramakrishna, M. V. *J. Chem. Phys.* **1996**, *105*, 3612.
(20) Wang, L.-W.; Zunger, A. *Phys. Rev. B* **1996**, *53*, 9579.
(21) Mizel, A.; Cohen, M. L. *Phys. Rev. B* **1997**, *56*, 6737.
(22) Ren, S.-Y.; Ren, S.-F. *J. Phys. Chem. Solids* **1998**, *59*, 1327.
(23) Wang, L.-W.; Zunger, A. *J. Phys. Chem. B* **1998**, *102*, 6449.
(24) Leung, K.; Pokrant, S.; Whaley, K. B. *Phys. Rev. B* **1998**, *57*, 12291.
(25) Rabani, E.; Hetényi, B.; Berne, B. J.; Brus, L. E. *J. Chem. Phys.* **1999**, *110*, 5355.
(26) Pérez-Conde, J.; Bhattacharjee, A. K. *Solid State Commun.* **1999**, *110*, 259.
(27) Franceschetti, A.; Fu, H.; Wang, L. W.; Zunger, A. *Phys. Rev. B* **1999**, *60*, 1819.
(28) Leung, K.; Whaley, K. B. *J. Chem. Phys.* **1999**, *110*, 11012.
(29) Pokrant, S.; Whaley, K. B. *Eur. Phys. J. D* **1999**, *6*, 255.
(30) Eichkorn, K.; Ahlrichs, R. *Chem. Phys. Lett.* **1998**, *288*, 235.
(31) Deglmann, P.; Ahlrichs, R.; Tsereteli, K. *J. Chem. Phys.* **2002**, *116*, 1585.
(32) Troparevsky, M. C.; Chelikowsky, J. R. *J. Chem. Phys.* **2001**, *114*, 943.
(33) Troparevsky, M. C.; Kronik, L.; Chelikowsky, J. R. *Phys. Rev. B* **2001**, *65*, 033311.
(34) Porezag, D.; Frauenheim, Th.; Köhler, Th.; Seifert, G.; Kaschner, R. *Phys. Rev. B* **1995**, *51*, 12947. Seifert, G.; Porezag, D.; Frauenheim, Th. *Int. J. Quantum Chem.* **1996**, *58*, 185.
(35) Elstner, M.; Porezag, D.; Jungnickel, G.; Elsner, J.; Haugk, M.; Frauenheim, Th.; Suhai, S.; Seifert, G. *Phys. Rev. B* **1998**, *58*, 7260. Frauenheim, Th.; Seifert, G.; Elstner, M.; Niehaus, T. A.; Köhler, C.; Amkreutz, M.; Sternberg, M.; Hajnal, Z.; di Carlo, A.; Suhai, S. *J. Phys.: Condens. Matter* **2002**, *14*, 3015.
(36) Niehaus, T. A.; Suhai, S.; Della Sala, F.; Lugli, P.; Elstner, M.; Seifert, G.; Frauenheim, Th. *Phys. Rev. B* **2001**, *63*, 085108.
(37) Hohenberg, P.; Kohn, W. *Phys. Rev.* **1964**, *136*, B864.
(38) Kohn, W.; Sham, L. J. *Phys. Rev.* **1965**, *140*, A1133.
(39) Casida, M. E. In *Recent Advances in Density Functional Methods*; Chong, D. P., Ed.; World Scientific: Singapore, 1995; Part 1, p 155.
(40) Casida, M. E. In *Recent Developments and Applications of Modern Density Functional Theory*; Seminario, J. M., Ed.; Theoretical and Computational Chemistry; Elsevier Science: Amsterdam, 1996; Vol. 4, p 391.
(41) In *Atomic and Molecular Physics*; Madelung, O., Schulz, M., Eds.; Landolt−Börnstein Numerical Data and Functional Relationships in Science and Technology, New Series III: Crystal and Solid: Semiconductors; Springer: Berlin, 1986; Vol. 22a, p 194.
(42) Fu, H.; Zunger, A. *Phys. Rev. B* **1997**, *56*, 1496.
(43) de Heer, W. A.; Selby, K.; Kresin, V.; Masui, J.; Vollmer, M.; Châtelain, A.; Knight, W. D. *Phys. Rev. Lett.* **1987**, *59*, 1805.
(44) Fabian, J.; Diaz, L. A.; Seifert, G.; Niehaus, T. *J. Mol. Struct.: THEOCHEM*, in press.
(45) Bawendi, M. G.; Wilson, W. L.; Rothberg, L.; Carroll, P. J.; Jedju, T. M.; Steigerwald, M. L.; Brus, L. E. *Phys. Rev. Lett.* **1990**, *65*, 1623.
(46) Ramaniah, L. M.; Nair, S. V. *Phys. Rev. B* **1993**, *47*, 7132.
(47) Murray, C. B.; Norris, D. J.; Bawendi, M. G. *J. Am. Chem. Soc.* **1993**, *115*, 8706.
(48) Soloviev, V. N.; Eichhöfer, A.; Fenske, D.; Banin, U. *J. Am. Chem. Soc.* **2000**, *122*, 2673.